



Tracking-based Experiments in Double Beta Decay

R. Saakyan^a

^a*Department of Physics and Astronomy, University College London, Gower Street, LONDON, WC1E 6BT UK*

Abstract

Neutrinoless double beta decay is the most sensitive way to test full lepton number violation and probe the nature of neutrino mass. Tracking based double beta decay experiments observe the process by reconstructing the topology of the event. This method provides a powerful background rejection and "smoking gun" evidence for the process. This report focuses on the results obtained with the currently running NEMO3 experiment and the status of its successor, the SuperNEMO project. The status of two projects based on gaseous ¹³⁶Xe, NEXT and EXO-Gas, and a brief review of the DCBA experiment are also presented.

Keywords:

neutrino mass, double beta decay, topological signature

1. Introduction

Neutrinoless double beta decay ($0\nu\beta\beta$) is the only practical way to understand the nature of the neutrino (Dirac or Majorana particle) and to observe full lepton number violation required by most GUT schemes. It may also turn out to be the only way to measure the absolute neutrino mass in a laboratory environment. The $0\nu\beta\beta$ half-life is given by

$$[T_{1/2}^{0\nu}(A, Z)]^{-1} = |\eta|^2 \cdot |M^{0\nu}(A, Z)|^2 \cdot G^{0\nu}(Q_{\beta\beta}, Z) \quad (1)$$

where η is a lepton number violating parameter, $M^{0\nu}$ is the nuclear matrix element (NME) and $G^{0\nu}$ is a known phase space factor. The mechanism most commonly discussed is the one where a light Majorana neutrino is exchanged in which case $|\eta| = \langle m_\nu \rangle$. However many other mechanisms are possible: V+A currents, Majoron emission, R-parity violating SUSY, to name a few [1].

Observation of the $\beta\beta$ decay topological signature, the angular correlations of the emitted electrons and their individual energies, provides a way of discriminating the underlying physics mechanism. In addition the $\beta\beta$ event topology observed in a tracking detector provides an unambiguous signature of the process ("smoking gun").

Due to topology identification tracking $\beta\beta$ experiments can carry out precision measurements of the $2\nu\beta\beta$ decay, a second order electroweak interaction allowed in the standard model. Measurement of $2\nu\beta\beta$ is important because it is an irreducible background component to 0ν mechanisms. Moreover $2\nu\beta\beta$ half-life measurements allow experimental determination of the NME for this process ($M^{2\nu}$), which leads to the development of theoretical models for NME calculations for $2\nu\beta\beta$ and $0\nu\beta\beta$ [2].

This report will focus on the results obtained with the currently running NEMO3 experiment and the status of its successor, the SuperNEMO project. The status of two projects based on gaseous ¹³⁶Xe, NEXT and EXO-Gas, and a brief review of the DCBA experiment are also presented.

2. NEMO3

The NEMO3 detector is located in the Modane underground laboratory (LSM) in the Frejus tunnel between France and Italy. The underground laboratory is shielded from cosmic rays by 1700m of rock overburden, corresponding to 4800m of water equivalent.

2.1. The NEMO3 Detector

The NEMO3 detector is a cylinder made of detector segments containing different samples of double beta decay enriched isotopes. The source foils of $\beta\beta$ emitters were constructed from either a metal film or powder bound by an organic glue to mylar strips. The source hangs between two concentric cylindrical tracking volumes consisting of open octagonal drift cells operating in Geiger mode (6180 cells). The tracking detector has an average position resolution of $\sigma_{\perp} = 0.3\text{mm}$ (transverse) and $\sigma_{\parallel} = 0.8\text{cm}$ (longitudinal).

The external walls of these tracking volumes are covered by a calorimeter made of large blocks of plastic scintillator (1940 blocks in total) coupled to low radioactivity 3" and 5" PMTs. The energy resolution of the NEMO3 calorimeter is $\Delta E/E = 14 - 17\%/\sqrt{E(\text{MeV})}$. The electron tracks curve under the influence of a 25G magnetic field to reject pair production events. The detector is substantially shielded from external gamma ray background by 20cm of low activity iron and 30cm of water with boron acid to suppress the neutron flux.

There are seven different isotopes studied in NEMO3. The two isotopes with the largest mass are ^{100}Mo (6.9kg) and ^{82}Se (0.93kg). The other five isotopes are ^{130}Te (620g, 454g in the enriched and 166g in the natural Te source foils), ^{116}Cd (405g), ^{150}Nd (37g), ^{96}Zr (9.4g), ^{48}Ca (7g) which are used for $2\nu\beta\beta$ decay and background studies. NEMO3 has been collecting data since February 2003.

The $\beta\beta$ events are selected by requiring two reconstructed electron tracks with a curvature corresponding to a negative charge, originating from a common vertex in the source foil. Such a clear topological signature allows unambiguous reconstruction of $\beta\beta$ events and a very powerful background rejection (Figure 1).

A radon trapping facility was installed at LSM in October 2004. This reduced the radon activity around the detector by three orders of magnitude while the radon activity inside the tracking chamber was reduced by a factor of ~ 6 . The installation of this facility subdivided the NEMO3 data taking period into two phases. The average radon activity inside the tracking chamber during Phase 1 (February 2003 – September 2004) was 35mBq/m^3 , while in Phase 2 (December 2004 – present) it was reduced to 6mBq/m^3 . A full description of the NEMO3 detector and its performance can be found in [3].

2.2. NEMO3 Results

The tracking plus calorimetry technique employed in NEMO3 provides an accurate and efficient identi-

fication of background events. A comprehensive background model has been built using event topologies and energy distributions. It is described in detail in [4] together with event selection criteria used to identify background and signal events. Measurements of the $2\nu\beta\beta$ decay half-lives have been performed with unprecedented precision for the seven isotopes studied in NEMO3. The most precise measurement was obtained for ^{100}Mo corresponding to the electron spectra shown in Figure 1. The spectra shown are obtained with an exposure of $24\text{ kg}\times\text{yrs}$ of the Phase 2 period. The signal-to-background ratio is ~ 76 yielding the result: $T_{1/2}^{2\nu} = [7.17 \pm 0.01(\text{stat}) \pm 0.54(\text{sys})] \times 10^{18}\text{yr}$, in excellent agreement with previous (Phase 1) result published in [5].

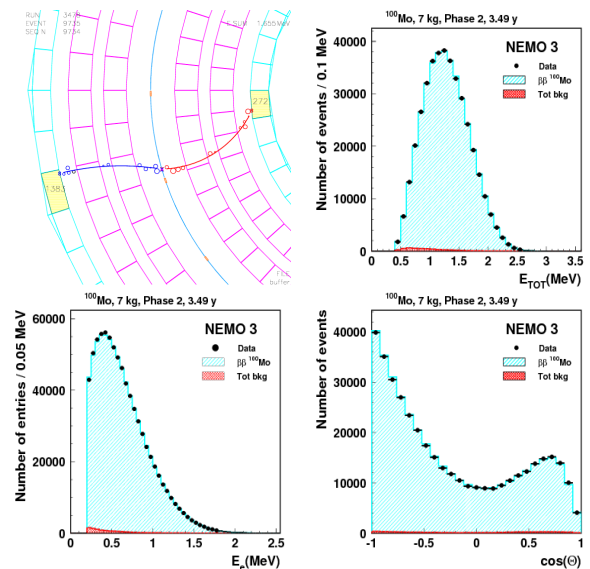


Figure 1: NEMO3 ^{100}Mo results. Top left: An event display showing a $\beta\beta$ candidate event; Top right: Energy sum distribution of two electrons emitted from the ^{100}Mo source and passed $\beta\beta$ selection criteria ($\beta\beta$ events); Bottom left: Single electron energy distribution for ^{100}Mo $\beta\beta$ events; Bottom right: The angle between the two electrons for ^{100}Mo $\beta\beta$ events.

The distribution of the two electron energy sum around the $Q_{\beta\beta}$ of ^{100}Mo was used to search for the $0\nu\beta\beta$ decay. No evidence for $0\nu\beta\beta$ has been observed, therefore a limit has been set using log-likelihood ratio test statistics described in [6]. For the Majorana mass mechanism the result is: $T_{1/2}^{0\nu} > 1.0 \times 10^{24}\text{yr}$ at 90% CL, which corresponds to an upper bound on the Majorana neutrino mass of $\langle m_{\beta\beta} \rangle < (0.47 - 0.96)\text{ eV}$ where the range reflects the spread in the NME calculations taken from [7]. Other mechanisms of $0\nu\beta\beta$ decay have been investigated. V+A currents in the elec-

troweak Lagrangian lead to $T_{1/2}^{0\nu} > 5.4 \times 10^{23} \text{ yr}$ at 90% CL giving an upper bound on the right-handed current admixture parameter, $\lambda < 1.4 \times 10^{-6}$. The $0\nu\beta\beta$ decay proceeding through a Majoron emission yields $T_{1/2}^{0\nu} > 2.1 \times 10^{22} \text{ yr}$ at 90% CL. We note that this limit corresponds to the world's most stringent constraint on the Majoron-neutrino coupling, $\eta < 0.5 \times 10^{-4}$.

The $\beta\beta$ decay of ^{100}Mo to excited states of ^{100}Ru was investigated with the Phase-I data and reported earlier in [8]. Data analysis using the total data sample is in progress and a result with a much improved sensitivity will be published soon.

Table 1 shows a summary of the main results obtained with 7 isotopes in NEMO3. These are the most precise measurements of the $2\nu\beta\beta$ half-lives for these isotopes. In the case of ^{130}Te this is the first 5σ observation of its $2\nu\beta\beta$ process in a direct experiment. The ^{130}Te measurement provides a reference point to a long dispute between geochemical experiments that yielded inconsistent results for the ^{130}Te half-life [9, 10]. Extracted NME values for the 7 isotopes (see Table 1) provide input for tuning NME calculation models.

Isotope	Mass, g	$T_{1/2}^{2\nu}$, yr	$M^{2\nu}$	$T_{1/2}^{0\nu}$, yr
^{100}Mo	6914	$(7.17 \pm 0.54) \times 10^{18}$	0.126 ± 0.006	$> 1 \times 10^{24}$
^{82}Se	932	$(9.6 \pm 1.0) \times 10^{19}$	0.049 ± 0.004	$> 3.2 \times 10^{23}$
^{130}Te	454	$(7.0 \pm 1.4) \times 10^{20}$	0.0173 ± 0.0025	$> 1.0 \times 10^{23}$
^{116}Cd	405	$(2.88 \pm 0.17) \times 10^{19}$	0.0685 ± 0.0025	$> 1.3 \times 10^{23}$
^{150}Nd	37	$(9.11 \pm 0.68) \times 10^{18}$	0.030 ± 0.002	$> 1.8 \times 10^{22}$
^{96}Zr	9.4	$(2.35 \pm 0.21) \times 10^{19}$	0.049 ± 0.002	$> 9.2 \times 10^{21}$
^{48}Ca	6.99	$(4.4 \pm 0.64) \times 10^{19}$	0.0238 ± 0.0015	$> 1.3 \times 10^{22}$

Table 1: Main results obtained with 7 isotopes studied in NEMO3. Combined statistical and systematic errors are shown for $T_{1/2}^{2\nu}$. $T_{1/2}^{0\nu}$ limits are shown at 90% CL. The NME values, $M^{2\nu}$, are scaled by the electron rest mass.

3. SuperNEMO

SuperNEMO aims to extend and improve the successful NEMO3 technology. It will extrapolate NEMO3 by one order of magnitude by studying about 100kg of $\beta\beta$ isotope(s). The detector's ability to measure any $\beta\beta$ isotope and reconstruction of the topological signature of the decay are distinct features of SuperNEMO. The baseline isotope choice for SuperNEMO is ^{82}Se . However other isotopes are possible. In particular, ^{150}Nd and ^{48}Ca are being studied.

3.1. SuperNEMO detector and sensitivity

The SuperNEMO design envisages twenty identical modules, each housing 5 kg of isotope. A schematic

design of a SuperNEMO module is shown in Figure 2. The module is 6m long, 4m high and 2m wide with the source foil to calorimeter wall distance of 44cm. The source is a thin ($40\text{mg}/\text{cm}^2$) foil inside the detector. It is surrounded by a gas tracking chamber followed by calorimeter walls. The tracking volume contains 2000 wire drift cells operated in Geiger mode in a gas mixture of He (95%), Ar(1%) and ethyl alcohol (4%). The cells are arranged in nine layers parallel to the foil. The calorimeter is divided into 500 plastic scintillator blocks with a cross-section of $26\text{cm} \times 26\text{cm}$ coupled to low radioactive 8-inch PMTs. A 25G magnetic field is envisaged for SuperNEMO to reject positron events from external γ -background. The modules will be surrounded with ultra-pure water passive shielding. The detector will be located in a new extended LSM laboratory which is expected to become operational after 2013.

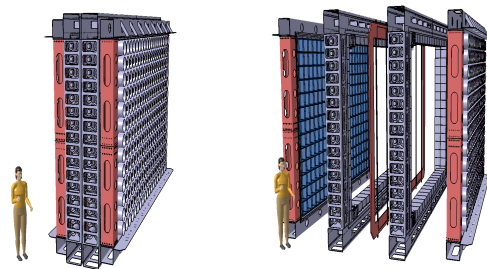


Figure 2: SuperNEMO Detector Module. Main detector sub-modules are shown on the right with a source foil frame in the centre, surrounded by two tracker sub-modules on either side and followed by two calorimeter sub-modules.

The sensitivity of SuperNEMO has been studied extensively with a full chain of GEANT-4 based simulation software and modelling the detector effects and backgrounds based on NEMO3 experience. Figure 3 shows the SuperNEMO physics reach as a function of the calorimeter energy resolution and background level. An exposure of $500 \text{ kg} \times \text{yr}$ gives a sensitivity for ^{82}Se of $T_{1/2}^{0\nu} > 10^{26} \text{ yr}$ at 90% CL corresponding to an upper bound on the effective Majorana neutrino mass of 50–100 meV.

The ability of SuperNEMO to study different isotopes and track the outgoing electrons provides the means to discriminate different underlying mechanisms for $0\nu\beta\beta$ by measuring the decay half-life and the electron angular and energy distributions. The potential of SuperNEMO to probe new physics scenarios of light Majorana neutrino exchange and right-handed currents is explored in detail in [11].

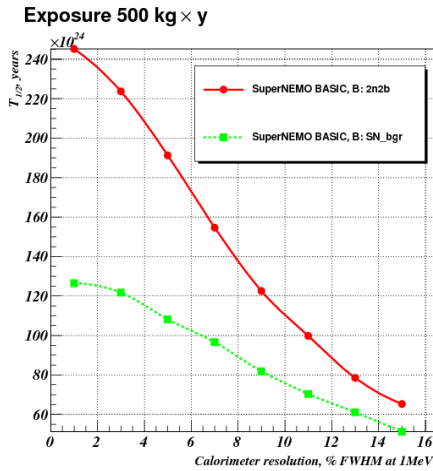


Figure 3: SuperNEMO $T_{1/2}^{0\nu}$ sensitivity with ^{82}Se as a function of the calorimeter energy resolution with a $2\nu\beta\beta$ only background (red) and target background levels (green).

3.2. SuperNEMO design study

An extensive R&D programme carried out between 2006–2010 has addressed three main challenges: improvement of the calorimeter energy resolution, radiopurity of the source foils, and optimisation of the tracker. The expected improvement in performance of SuperNEMO compared to NEMO3 is shown in Table 2.

Detector Parameter	NEMO3	SuperNEMO
Isotope/mass	7kg of ^{100}Mo	100 kg of ^{82}Se (or other)
Detector efficiency	18%	30%
^{208}Tl (in $\beta\beta$ source)	$\sim 100 \mu\text{Bq/kg}$	$\leq 2 \mu\text{Bq/kg}$
^{214}Bi (in $\beta\beta$ source)	$\leq 300 \mu\text{Bq/kg}$	$\leq 10 \mu\text{Bq/kg}$
^{222}Rn (in tracker)	$\sim 5 \text{ mBq/m}^3$	$\leq 0.15 \text{ mBq/m}^3$
Calorimeter FWHM at $Q_{\beta\beta} = 3 \text{ MeV}$	8%	4%
$T_{1/2}^{0\nu}$, 90% CL	$1.5 \times 10^{24} \text{ yr}$	$1.0 \times 10^{26} \text{ yr}$

Table 2: Expected improvements in SuperNEMO performance compared to NEMO3.

A good energy resolution is important for discriminating the $0\nu\beta\beta$ peak in the energy sum of the two electrons from the background of the $2\nu\beta\beta$ decay. A large number of studies have been carried out to investigate the material, size, shape and coating of the calorimeter blocks as well as performance and intrinsic activity of the PMTs. Test bench studies have been backed up by optical simulations which were also verified on the NEMO3 running calorimeter [12]. As a result the feasibility to reach the required energy resolution of $7 - 8\% / \sqrt{E(\text{MeV})}$ with a large (26cm \times 26cm \times 15cm) block has been experimentally demonstrated. A basic building block of the SuperNEMO calorimeter will have

a large PVT-based scintillator block coupled to a low radioactive high-QE 8" R5912MOD Hamamatsu PMT.

The SuperNEMO tracker consists of wire drift cells operated in Geiger mode. Each cell has a $40 \mu\text{m}$ stainless steel central anode wire surrounded by 12 $50 \mu\text{m}$ ground wires, with cathode pickup rings at both ends. Over 400,000 wires will have to be strung, crimped and terminated for all 20 modules. The large number of wires and strict radiopurity requirements have led to the need of automated wiring. A dedicated wiring robot has been developed for mass production of the cells. The tracking detector design has been optimised for automated wiring, high detection efficiency and reliability. The required spatial resolution (0.7mm radial and 1cm longitudinal) for individual tracker hits have been demonstrated with a 90-cell and a number of single-cell and 9-cell prototypes.

The most stringent radiopurity requirements apply to the SuperNEMO source foil (see Table 2). In order to evaluate ultra-low contaminations of ^{208}Tl and ^{214}Bi in the foils a dedicated BiPo detector has been developed which exploits the signature of an electron followed by a delayed alpha particle emitted in the $^{214}\text{Bi} \rightarrow ^{214}\text{Po}$ and $^{212}\text{Bi} \rightarrow ^{212}\text{Po}$ transitions of the ^{238}U and ^{232}Th series respectively. The target sensitivity of $\leq 10 \mu\text{Bq/kg}$ has been reached with the first prototype BiPo1 detector [13]. A new BiPo-3 detector is being constructed to measure the source foils for the SuperNEMO demonstrator module (see 3.3).

3.3. SuperNEMO Demonstrator and schedule outline

Having successfully completed the R&D stage the SuperNEMO collaboration has commenced the construction of the first module, the demonstrator. The main goals of the demonstrator are: to demonstrate feasibility of mass production of detector components under ultra-low background conditions; to measure backgrounds especially from radon emanation; to finalise the detector design; to produce a competitive $\beta\beta$ physics result. To accomplish the latter goal on a competitive time scale the demonstrator module will house 7 kg of the ^{82}Se isotope. The construction and commissioning of the demonstrator will be completed in 2013 with data taking expected to commence in the second half of 2013. The module will be located either in the extended LSM laboratory or in the existing cavern if the new laboratory is not ready by then. The sensitivity of the demonstrator after 17 kg \times yr of exposure is $6.5 \times 10^{24} \text{ yr}$ (90% CL) which is equivalent to $3 \times 10^{25} \text{ yr}$ obtained with ^{76}Ge assuming equal NME and using the phase space ratio for these isotopes. This sensitivity will be

reached by the end of 2015 and will match the sensitivity of the GERDA-Phase1 experiment [14] allowing experimental verification of a recent claim of evidence for $0\nu\beta\beta$ [15].

The modular design of SuperNEMO makes it possible to proceed with construction and data taking in parallel. The full detector construction is expected to start in 2014 (in parallel with the demonstrator running). The 500 kg \times yr exposure will be reached in 2019 pushing the sensitivity to the effective Majorana neutrino mass down to 50–100 meV.

4. Other tracking $\beta\beta$ experiments

Other projects exploiting the $\beta\beta$ signature reconstruction include experiments based on a high-pressure Xenon TPC (NEXT and EXO-Gas) and the DCBA experiment using magnetic field to reconstruct the momenta of $\beta\beta$ electrons.

4.1. Xenon TPC: NEXT and EXO-Gas

A high-pressure gaseous Xenon (HPGXe) TPC offers a potentially promising tool to search for $0\nu\beta\beta$ decay. In this case Xe serves as the source and detector medium at the same time (the $\beta\beta$ isotope is ^{136}Xe). Unlike in liquid Xe, the $\beta\beta$ topological signature can be reconstructed in gaseous Xe. Although due to multiple scattering the electron tracks are not as clear as in NEMO3/SuperNEMO and therefore angular correlations can not be studied one can nevertheless identify electron tracks. Ionisation density information can be used for particle identification. Multiple-site events can also be efficiently rejected providing an important handle on background suppression. An example simulation event of a track produced by a $\beta\beta$ event in a HPGXe TPC at 10 bar is shown in Figure 4. Two characteristic “blobs” at the end of the tracks can be used to discriminate two-electron from single electron events.

The basic detection concept of Xe HP-TPC is as follows. An ionising event in the detector will cause a scintillation flash which will be detected by light sensors and serve as the trigger and time zero signal. Ionisation electrons will drift toward an anode under an electric field. Once they are close to the anode they enter a strong field region where they will give rise to light through the electroluminescence (EL) process. The concept was suggested in [16] where it was shown that this approach can potentially lead to a very good energy resolution. An alternative solution is to use charge amplification with Micromegas [17] detectors instead of the EL signal.

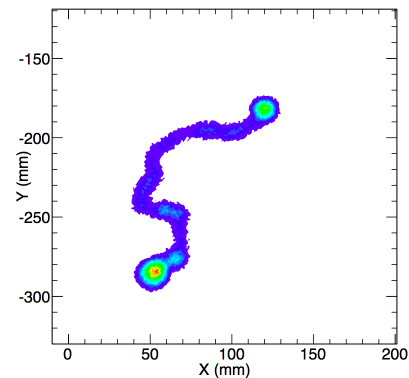


Figure 4: A simulated 2e event in a HPGXe TPC at 10 bar.

The NEXT (Neutrino Experiment with a Xenon TPC) experiment is designed in two phases. The first phase envisages an operation of 10kg Xe TPC at 5 to 10 bar to prove basic technology principles, demonstrate the background suppression methods and measure the $2\nu\beta\beta$ half-life of ^{136}Xe . In the second phase the collaboration plans to have a 100 kg detector enriched in ^{136}Xe to search for its $0\nu\beta\beta$ decay. The experiment will be located in the Canfranc underground laboratory in Huesca (Spain). An R&D programme is underway to demonstrate feasibility of the detector technology for low background physics. Both EL and Micromegas approaches are pursued in parallel. At the end one of them will be chosen for the final detector depending on its performance with respect to energy resolution, suitability for low background environment and robustness. MC simulations of the NEXT physics reach have been carried out with a number of assumptions on the detector performance indicating a sensitivity to the Majorana neutrino effective mass of ~ 0.1 eV after a 500 kg \times yr exposure.

The EXO collaboration is pursuing an R&D programme to develop a gaseous Xe TPC in parallel with its baseline detector concept based on liquid Xenon. The EL signal will be used to detect the primary ionisation signal and the detector will be filled with pure Xenon (no quenching). A distinctive feature of the EXO experiment is the idea of detecting the ^{136}Ba ion, the daughter of the ^{136}Xe $\beta\beta$ decay. This is a very challenging task but, if successful, could in principle eliminate all backgrounds apart from the tail of the $2\nu\beta\beta$ distribution. A gaseous detector opens new ways to try to identify the daughter barium ion using new techniques developed for radioactive ion beams for ion extraction. Further development of the gaseous detector will depend on the results obtained with the EXO-200 detector that will run

with liquid Xenon and no barium tagging [18].

4.2. DCBA experiment

The DCBA (Drift Chamber Beta-ray Analyser) experiment uses a drift chamber in a uniform magnetic field to reconstruct the momenta of the electrons. The detector is only sensitive to charged particles, thus direct gamma-ray background is eliminated. Positrons are distinguished through the opposite sign of the track curvature while α -particles are identified thanks to their high momentum values and high ionisation density. The detector has been developed at KEK (Japan) and a test prototype DCBA-T2 has been constructed and operated to demonstrate the basic technology. A more detailed description of the detector performance can be found in [19]. A new prototype DCBA-T3 is under construction at KEK. It will have a magnetic field of 2 kG and its main aim is to improve energy resolution reaching $\text{FWHM} = 6\%$ at 1 MeV. The detector can host different isotopes in a foil form in the middle of the detector. The main focus is on ^{150}Nd . It is expected that DCBA-T3 will be able to measure the half-life of the ^{150}Nd $2\nu\beta\beta$ decay.

5. Summary

Neutrinoless double beta decay is a powerful way of addressing the most fundamental particle physics questions including lepton number violation and the absolute scale of neutrino mass. Tracking based detectors offer a unique approach to the detection of the $\beta\beta$ process in which the topology of the decay is fully reconstructed. Apart from producing a clear “smoking gun” signature of the process these detectors offer a superior background rejection capability. As such, they are complementary to pure calorimeter experiments such as GERDA, CUORE, SNO+. Moreover, as demonstrated by NEMO3 and SuperNEMO, once the process is detected the measurement of the individual energies of the electrons emitted in the decay and the angular distribution between them may allow the underlying physics mechanism of $0\nu\beta\beta$ to be disentangled.

References

- [1] F.T. Avignone III, S.R. Elliott and J. Engel, Rev. Mod. Phys. 80 (2008) 481.
- [2] V.A. Rodin *et al.*, Nucl. Phys. A 766 (2006) 107.
- [3] R. Arnold *et al.*, Nucl. Instr. Meth. A 536 (2005) 79.
- [4] J. Argyriades *et al.*, Nucl. Instr. Meth. A 606 (2009) 449.
- [5] R. Arnold *et al.*, Phys. Rev Lett. 95 (2005) 182302.
- [6] Th. Junk, Nucl. Instr. Meth. A 434 (1999) 435.
- [7] M.Kortelainen and J.Suhonen, Phys.Rev. C 76 (2007) 024315; F.Simkovic *et al.*, Phys.Rev. C 77 (2008) 045503.
- [8] R. Arnold *et al.*, Nucl. Phys. A 781 (2007) 209.
- [9] A.S. Barabash, Eur. Phys. J. A 8 (2000) 137.
- [10] A.P. Meshik *et al.*, Nucl. Phys. A 809 (2008) 275.
- [11] R. Arnold *et al.*, Eur. Phys. J. C Eur. Phys. J. C 70 (2010) 927.
- [12] J. Argyriades *et al.*, Nucl. Instr. Meth. A 625 (2011) 20.
- [13] J. Argyriades *et al.*, Nucl. Instr. Meth. A 622 (2010) 120.
- [14] K. Kröninger for the GERDA Collaboration J. Phys.Conf. Ser. 110 (2008) 082010.
- [15] H.V. Klapdor-Kleingrothaus and I.V.Krivoshchina, Mod. Phys. Lett. A 21 (2006) 1547.
- [16] D. Nygren, Nucl. Instr. Meth. A 581 (2007) 632.
- [17] Y. Giomataris *et al.*, Nucl. Instr. Meth. A 376 (1996) 29.
- [18] L.J. Kaufman for EXO Collaboration, J. Phys.Conf. Ser.203 (2010) 012067.
- [19] N Ishihara *et al.*, J. Phys.Conf. Ser.203 (2010) 012071.